EPJ Web of Conferences **81**, 01024 (2014)
DOI: 10.1051/epjconf/ 20148101024

Recent ATLAS results in the field of meson physics

Rui Wang[1,a]
on behalf of the ATLAS Collaboration

[1] *Department of Physics and Astronomy, University of New Mexico, 1919 Lomas Blvd NE, Albuquerque, NM, US, 87131*

Abstract. Recent results on flavor physics are presented, using data from the ATLAS detector. The $\Upsilon(nS)$ and charmonium inclusive production cross sections are discussed. J/ψ production associated with a W vector boson is presented. An inclusive analysis of B^+ meson production is shown. Results on the production of heavy quarkonia are complemented by the measurement of inclusive ϕ meson production. The latest information on heavy flavor spectroscopy and searches for new physics using B-meson rare decays is also covered. These results are based on data samples collected during the 2011 and 2012 LHC running periods.

1 The ϕ(1020) production cross section measurement

As a theory of the physics at high momentum transfer, perturbative quantum chromodynamics (pQCD) is very successful. However, for interactions at low momentum transfers, there is no single best model. The $\phi(1020)$ meson is produced in hard scatters during pp interactions as well as in hadronisation. Therefore, accurate measurements of $\phi(1020)$ meson production can be used to tune phenomenological fragmentation models.

The $\phi(1020)$ meson production is measured using 383 μb^{-1} of 7 TeV data collected in 2010 [1] using the ATLAS detector [2]. The $\phi(1020)$ is reconstructed using kaons identified by their energy loss in the pixel detector. The kaons are required to have transverse momentum $p_{\mathrm{T}} > 230$ MeV and total momentum $p < 800$ MeV. The analysis is restricted to the fiducial region $500 < p_{\mathrm{T}}(\phi) < 1200$ MeVand $|y(\phi)| < 0.8$, where y is rapidity. The integrated production cross section for $\phi(1020) \to K^+K^-$ is found to be $570 \pm 8(stat.) \pm 66(sys.) \pm 20(lumi.)$ μb. The differential cross sections are shown in Fig. 1 along with comparisons to various Monte Carlo (MC) based predictions. The `EPOS-LHC` and `PYTHIA6 DW` tunes give the best agreement.

2 W plus J/ψ associated production

The measurement of W plus J/ψ associated production can be used to test the relative contributions of the color singlet (CS) and color octet (CO) processes to $Q\bar{Q}$ production.

[a] e-mail: Rui.Wang@cern.ch

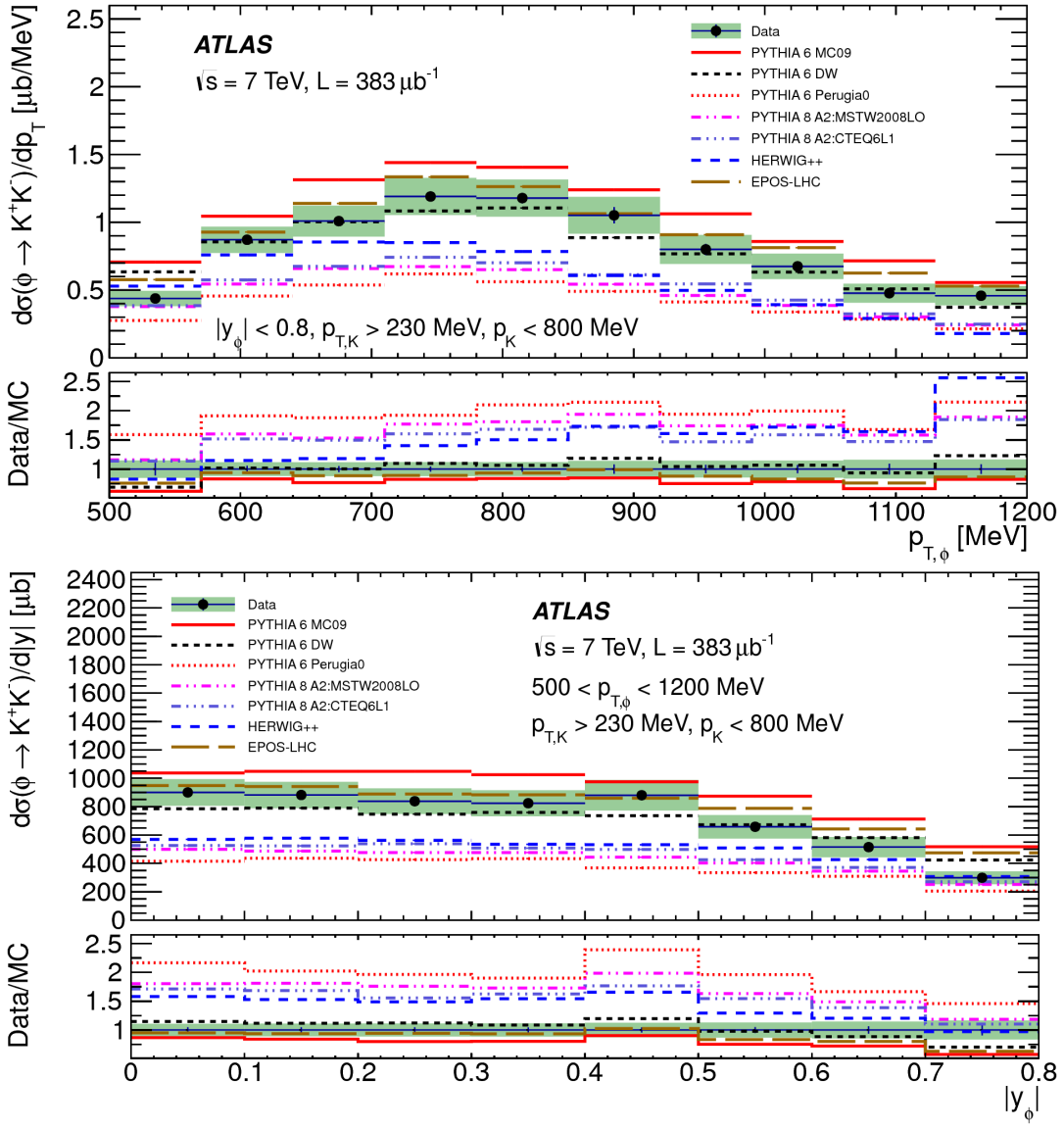

Figure 1: The $\phi(1020) \rightarrow K^+K^-$ cross section as a function of $p_{\mathrm{T}}(\phi)$ (left) and $|y(\phi)|$ (right), in the fiducial region of $500 < p_{\mathrm{T}}(\phi) < 1200$ MeV and $|y(\phi)| < 0.8$.

The measurement is based on 4.5 fb^{-1} of 7 TeV pp collision data collected by ATLAS in 2011 [3]. In total, $29.2^{+7.5}_{-6.5}$ prompt J/ψ plus W boson events are observed, corresponding to a signal 5.1 σ significance.

As shown in Fig. 2, left, these W boson plus prompt J/ψ events include both single parton scattering (SPS) events and double parton scattering (DPS) events. The DPS-subtracted rate appears to

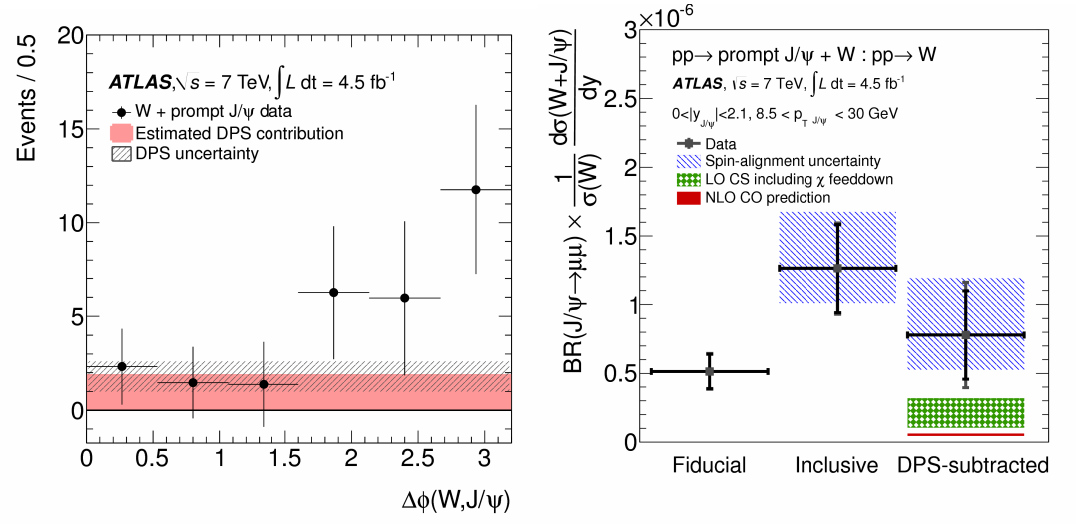

Figure 2: The sPlot-weighted azimuthal angle between the W and the J/ψ with a flat DPS contribution from MC overlaid (left). The W plus the J/ψ production cross-section ratio in the J/ψ fiducial region (Fiducial), after correction for J/ψ acceptance (Inclusive), and after subtraction of the double parton scattering component (DPS-subtracted) (right).

be dominated by CS (Fig. 2, right). However, both of the leading order (LO) CS and next-to-leading order (NLO) CO predictions are compatible with the measured result at the 2σ level.

3 Measurement of the $\chi_{c1,2}$ and $\psi(2S)$ production cross sections

Together with the J/ψ production cross section, χ_c and $\psi(2S)$ production cross section measurements can give a precise picture of the production of both prompt and non-prompt charmonium below the

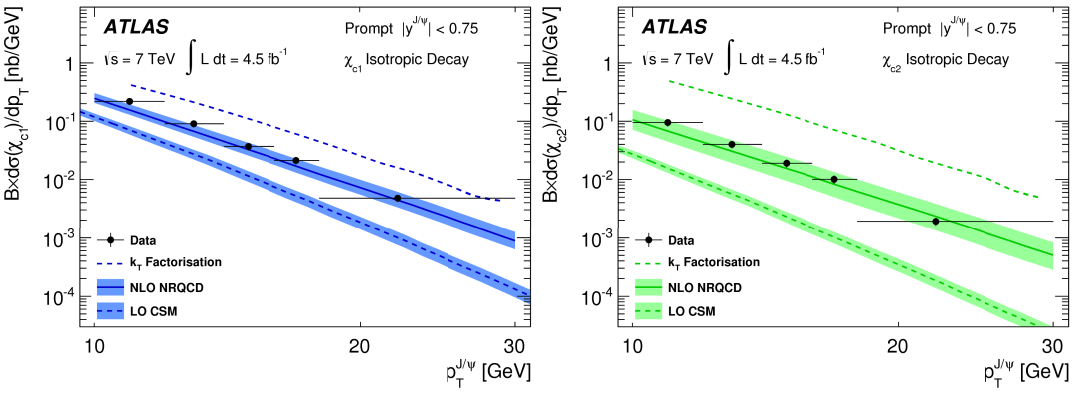

Figure 3: Differential cross-sections for prompt χ_{c1} (left) and χ_{c2} (right) production.

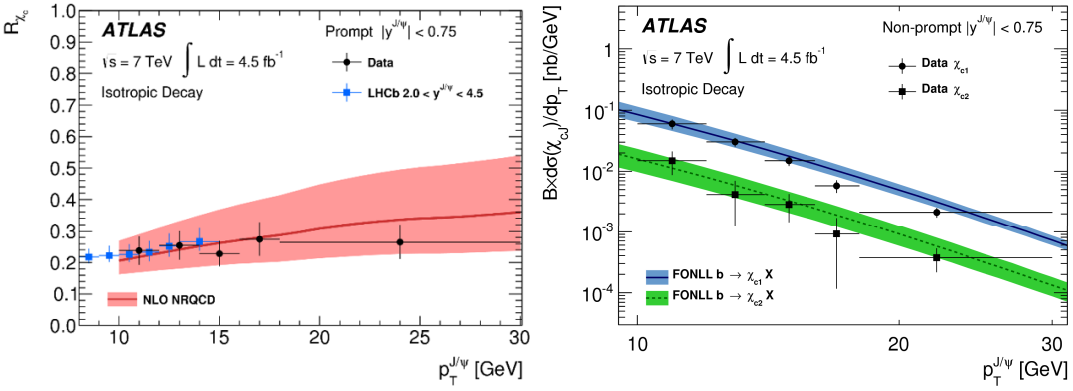

Figure 4: The fraction, R_{χ_c}, of prompt J/ψ events produced in χ_c decays is shown as a function of $p_{\mathrm{T}}^{J/\psi}$ (left). Differential cross-sections for non-prompt χ_{c1}, χ_{c2} (right).

$D\bar{D}$ threshold. The prompt production normally includes both direct production from pp collisions and production from decays of heavier charmonium states (the feed-down contribution). However, since $\psi(2S)$ is the highest state below the $D\bar{D}$ threshold, it has no contribution from higher states. The non-prompt production is contributed by the b hadron decays.

The $\chi_{c1,2} \rightarrow J/\psi\gamma$ production cross section is measured using 4.5 fb^{-1} of 7 TeV 2011 data in the ranges $10 < p_{\mathrm{T}}(J/\psi) < 30$ GeV and $|y(J/\psi)| < 0.75$ [4]. The $\psi(2S) \rightarrow J/\psi\pi\pi$ production cross section is measured using 2.1 fb^{-1} of 7 TeV 2011 data in the ranges $10 < p_{\mathrm{T}} < 100$ GeV and $|y| < 2.0$ [5]. The prompt production data are compared to different models (Fig. 3 and Fig. 5, left). NLO non-relativistic QCD (NRQCD) is compatible in both cases. The LO Color Singlet Model (CSM) underestimates the $\chi_{c1,2}$ production cross section and the $\psi(2S)$ production cross section. The k_{T} factorisation approach overestimates the $\chi_{c1,2}$ production cross section and underestimates the $\psi(2S)$

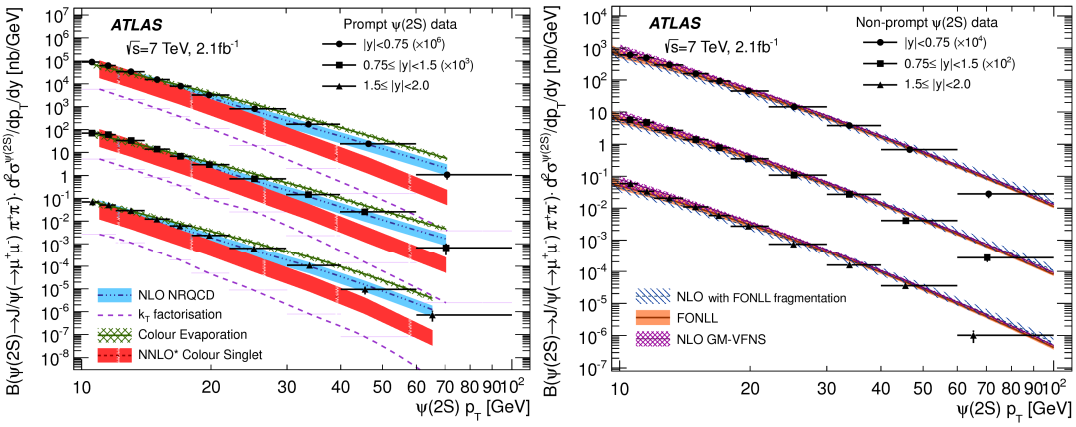

Figure 5: Differential cross-sections for prompt $\psi(2S)$ (left) and non-prompt $\psi(2S)$ (right) production.

production cross section. These suggest that higher-order corrections or CO contributions to the cross sections not included in either prediction may be important. Between 20% and 30% of prompt J/ψ mesons are produced in χ_{c1} feed-down (Fig. 4, left). As is shown in Fig. 4, right and Fig. 5, right, the non-prompt production data are compatible with the FONLL predictions.

4 Measurement of the $\Upsilon(nP)$ production cross section

As a complement to charmonium system studies, the Υ family allows more dependable theoretical calculations due to its members' larger masses. Additionally, the impact of spin-alignment uncertainties is mitigated. Like charmonium, Υ mesons are produced directly in pp collisions or from decay of excited states.

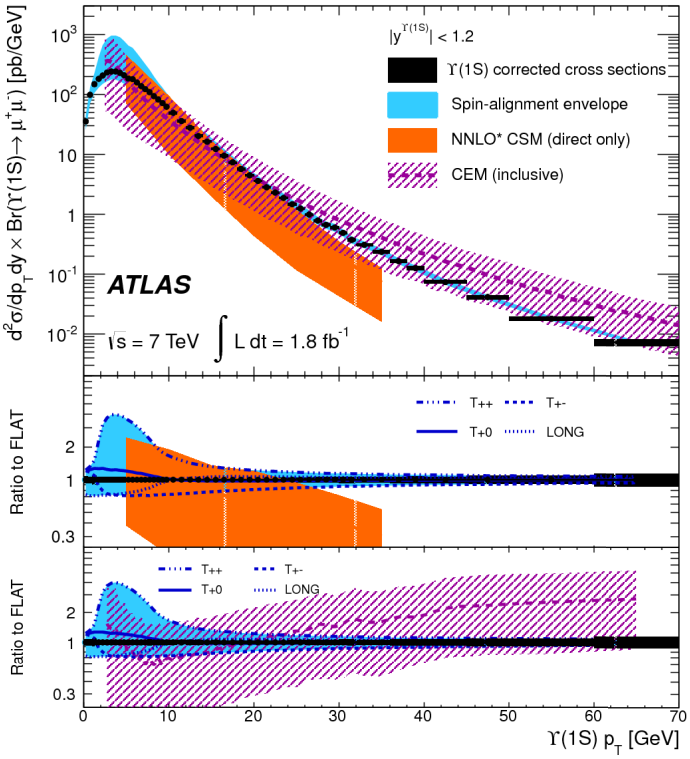

Figure 6: The $\Upsilon(1S)$ differential cross sections multiplied by the di-muon branching fraction, $d^2/dp_T dy \times \mathrm{Br}(\Upsilon \to \mu^+\mu^-)$.

The $\Upsilon(nS) \to \mu^+\mu^-$ production cross sections has been measured using 1.8 fb^{-1} of 7 TeV 2011 data collected by ATLAS in the ranges $p_T < 70$ GeV and $|y| < 2.25$ [6]. The integrated cross sections are found to be $\Upsilon(1S) = 8.01 \pm 0.02(stat.) \pm 0.36(sys.) \pm 0.31(lumi.)$ nb, $\Upsilon(2S) = 2.05 \pm 0.01(stat.) \pm 0.12(sys.) \pm 0.08(lumi.)$ nb, and $\Upsilon(3S) = 0.92 \pm 0.01(stat.) \pm 0.07(sys.) \pm 0.04(lumi.)$ nb. The differential cross sections (Fig. 6) can be well described by the CS model in the low p_T region but are underestimated in the high p_T region. The feed-down contribution has not been included into the CSM calculations. The color evaporation model (CEM) gives a better description, it includes the

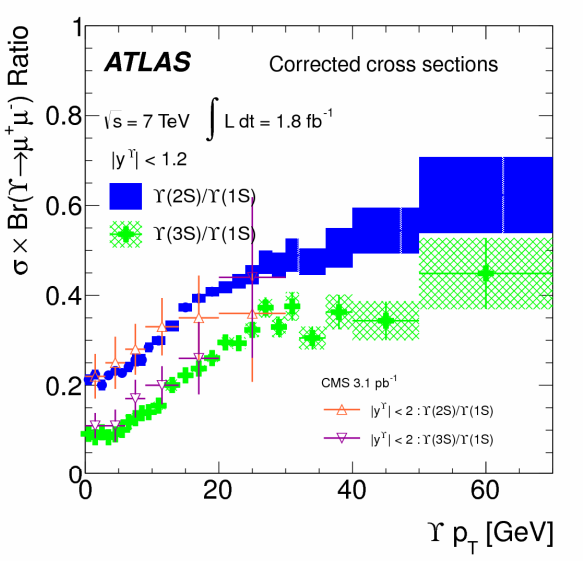

Figure 7: The ratios of differential $\Upsilon(2S)/\Upsilon(1S)$ and $\Upsilon(3S)/\Upsilon(1S)$ cross sections multiplied by the di-muon branching fractions versus Υ p_{T} in the central rapidity regions.

feed-down naturally. In Fig. 7, the increase in the p_{T} range of 5 GeV to 30 GeV may be related to the feed-down contribution.

5 Observation of a new χ_b state

$\chi_b(nP)$ states are sought using 4.9 fb^{-1} of ATLAS 2011 7 TeV data [7], through decay modes of $\chi_b(nP) \to \Upsilon(1S, 2S)\gamma$. In this measurement, a di-muon sample with requirments of $p_{\mathrm{T}} > 4$ GeV and

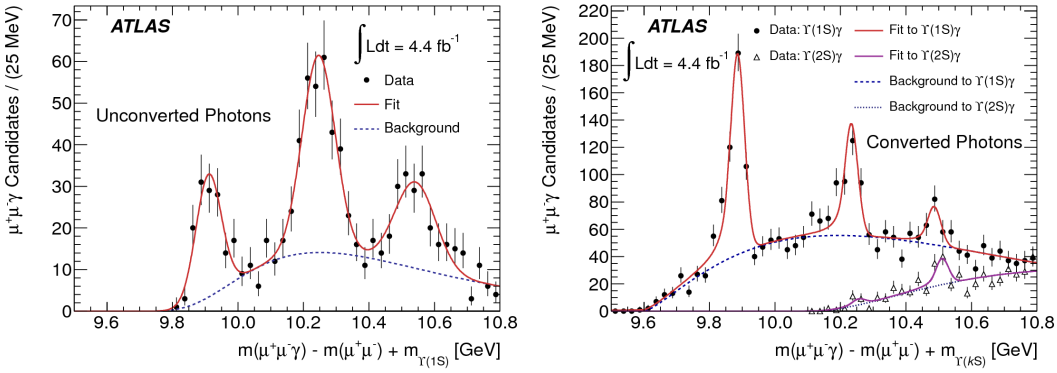

Figure 8: The mass distribution of $\chi_b \to \Upsilon(1S)\gamma$ candidates for unconverted photons (left) and the mass distributions of $\chi_b \to \Upsilon(kS)\gamma$ (k = 1, 2) candidates formed using converted photons (right).

pseudorapidity $|\eta| < 2.3$ for each muon has been used for $\Upsilon(1S, 2S)$ candidate selection. A photon is combined with each Υ candidate. Converted photons reconstructed from e^+e^- track pairs in the Inner Detector (ID) and unconverted photons reconstructed from electromagnetic calorimeter energy deposits are used.

As shown in the mass difference $(m(\mu^+\mu^-\gamma) - m(\mu^+\mu^-) + m_{PDG}(\Upsilon))$ distributions (Fig. 8), a new structure centered at mass $10.530 \pm 0.005(stat.) \pm 0.009(syst.)$ GeV is observed with a significance of more than 6σ in each of the unconverted and converted photon selections. This is interpreted as the $\chi_b(3P)$ state.

6 Angular analysis of $B_d \to K^{*0}(K^+\pi^-)\mu^+\mu^-$ events

The angular distributions of the $B_d \to K^{*0}(K^+\pi^-)\mu^+\mu^-$ four particle final state are sensitive to physics beyond the Standard Model (SM). Two important observables are the forward-backward asymmetry of the muons, A_{FB}, and the longitudinal polarization fraction of the K^{*0}, F_L. They can be extracted from the decay width which depends on the angle between those two muon momenta, the angle between the kaon and pion momenta, and the momentum transfer $q^2 = m^2(\mu^+\mu^-)$. The measurement uses 4.9 fb^{-1} of 7 TeV 2011 data recorded by ATLAS [8]. As shown in Fig. 9, both A_{FB} and F_L as measured by ATLAS are compatible with SM predictions and with other measurements.

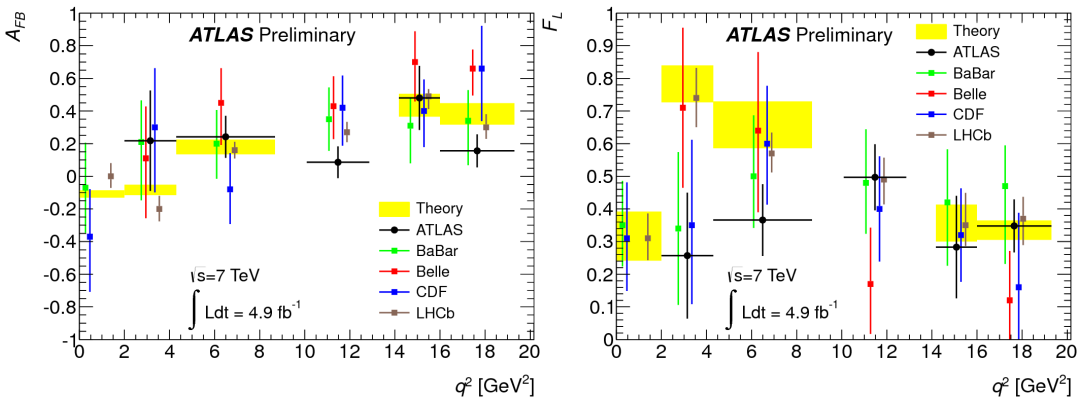

Figure 9: A_{FB} (left) and F_L (right) as a function of momentum transfer q^2. The SM theoretical predictions have been calculated for the limit of small vector meson energy and for the limit of large vector meson energy. No expectation is given for the central q^2 region. The q^2 bins corresponding to J/ψ and $\psi(2S)$ resonances are not filled.

7 Angular analysis of $B_s \to J/\psi\phi$ enents

The $B_s \to J/\psi\phi$ process is also sensitive to new physics beyond the SM. CP violation in this decay occurs due to interference between direct decays and decays occurring through $B_s^0 - \bar{B}_s^0$ mixing. The CP states are separated statistically through the time dependence of the decay and angular correlations among the final state particles. With 4.9 fb^{-1} of 7 TeV 2011 data, the ATLAS measurement of the CP violating weak phase is $\phi_s = 0.12 \pm 0.25(stat.) \pm 0.05(syst.)$ rad. The ATLAS measurement of the difference of widths of the heavy and light mass eigenstates is $\Delta\Gamma_s = 0.053 \pm 0.021(stat.) \pm 0.010(syst.)$ ps^{-1} [9]. Both are compatible with the SM predictions (Fig. 10).

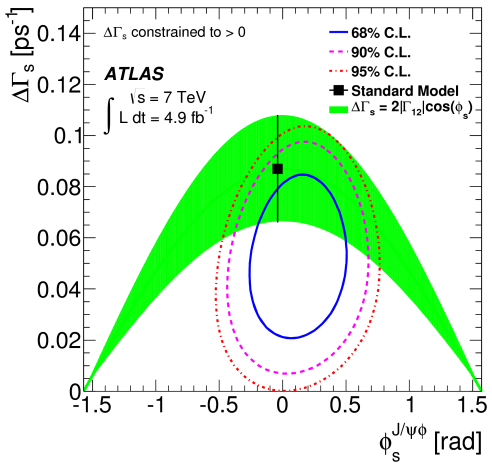

Figure 10: Likelihood contours in the ϕ_s - $\Delta\Gamma_s$ plane. The green band is the theoretical prediction of mixing-induced CP violation.

8 Search for the rare decay $B_s^0 \to \mu^+\mu^-$

Because flavor changing neutral currents (FCNC) are highly suppressed in the SM, the predicted branching ratio of $B_s^0 \to \mu\mu$ is quite small. It may be enhanced or reduced by new physics processes. At ATLAS, the decay has been searched with respect to a prominent reference decay ($B^+ \to J/\psi K^+$)

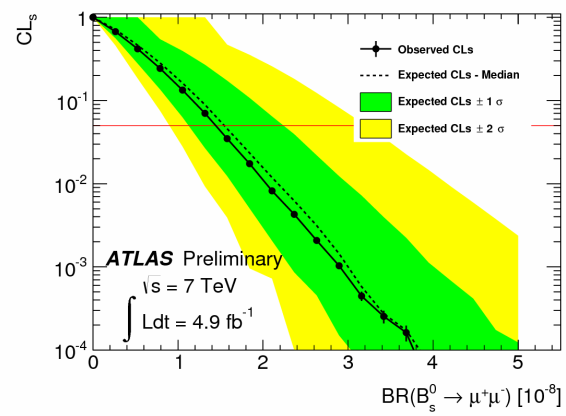

Figure 11: Observed confidence levels (CLs, circles) are shown as a function of BR($B_s^0 \to \mu^+\mu^-$). The 95% CL limit is indicated by the horizontal (red) line. The green and yellow bands correspond to $\pm 1\sigma$ and $\pm 2\sigma$ fluctuations on the expectation (dashed line).

using 4.9 fb^{-1} of 7 TeV 2011 data [10]. Six events in the signal region have been observed with 6.75 background events expected. Thus ATLAS sets a limit on the branching ratio at 1.5×10^{-8}@95% CL (Fig. 11).

9 Measurement of the B^+ production cross section

Precise measurements of B-hadron production cross sections in pp collisions at LHC can provide tests of QCD calculations for heavy-quark production at high center-of-mass energies and in wide p_{T} and y ranges. The $B^+ \to J/\psi K^+$ production cross section is measured using 2.4 fb^{-1} of early 2011 7

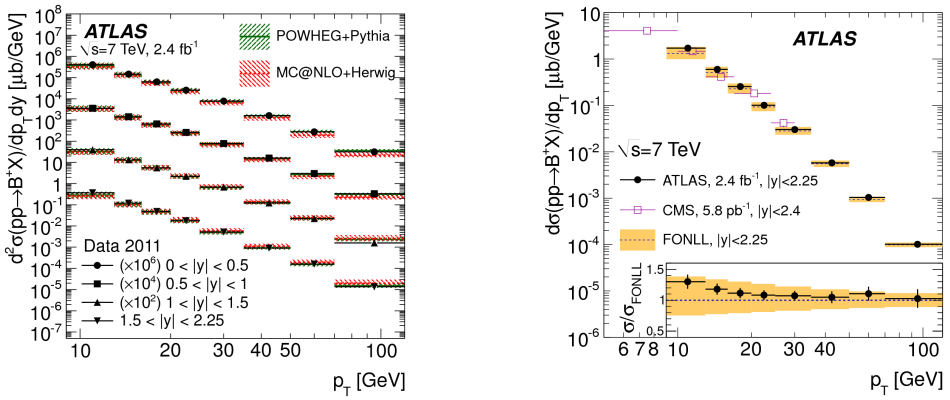

Figure 12: The doubly-differential cross-section for B^+ production as a function of p_{T} and y (left). The differential cross-section for B^+ production versus p_{T}, integrated over rapidity, compared with predictions using the FONLL calculation with a hadronization fraction $f_{b\to B^+}$ of $(40.1 \pm 0.8)\%$ (right).

TeV data [11]. The differential cross section in the kinematic range 9 GeV $< p_{\mathrm{T}} <$ 120 GeV and $|y| <$ 2.25 is shown in Fig. 12. Different model predictions have been compared to the measured data, and they are compatible within theoretical uncertainties.

10 B_c meson observation

The $B_c^{\pm}$ meson is a bound state of the two heaviest quarks able to form a stable state. Weak decays of

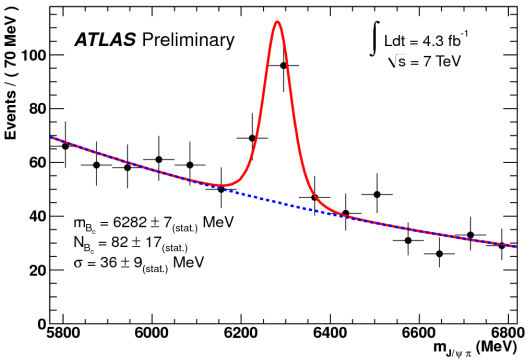

Figure 13: The invariant mass distribution of reconstructed $B_c^{\pm} \to J/\psi\pi^{\pm}$ candidates.

the $B_c^{\pm}$ meson provide a unique probe of heavy quark dynamics that is inaccessible to $b\bar{b}$ or $c\bar{c}$ bound states. The $B_c^{\pm}$ meson is reconstructed using 2011 7 TeV data in the decay mode $B_c \rightarrow J\psi\pi$ [12]. With 4.3 fb^{-1} data, 82 ± 17 B_c ground state mesons have been extracted using an unbinned maximum likelihood fit (Fig. 13). The B_c mass returned by the fit is 6282 ± 7 MeV, in agreement with the world average value.

References

[1] ATLAS Collaboration, Eur. Phys. J. **C74**, 2895 (2014).
[2] ATLAS Collaboration, JINST **3**, S08003 (2008).
[3] ATLAS Collaboration, JHEP **04**, 172 (2014).
[4] ATLAS Collaboration, JHEP **07**, 154 (2014).
[5] ATLAS Collaboration, JHEP **09**, 079 (2014).
[6] ATLAS Collaboration, Phys. Rev. D **87**, 052004 (2013).
[7] ATLAS Collaboration, Phys. Rev. Lett. **108**, 152001 (2012).
[8] ATLAS Collaboration, ATLAS-CONF-2013-038, https://cds.cern.ch/record/1537961.
[9] ATLAS Collaboration, Phys. Rev. D **90**, 052007 (2014).
[10] ATLAS Collaboration, ATLAS-CONF-2013-076, https://cds.cern.ch/record/1562934.
[11] ATLAS Collaboration, JHEP **10**, 042 (2013).
[12] ATLAS Collaboration, ATLAS-CONF-2012-028, https://cds.cern.ch/record/1430737.